Title	Silver nanoparticles mediate differential responses in keratinocytes and fibroblasts during skin wound healing
Author(s)	Liu, X; Lee, PY; Ho, CM; Lui, VCH; Chen, Y; Che, CM; Tam, PKH; Wong, KKY
Citation	Chemmedchem, 2010, v. 5 n. 3, p. 468-475
Issued Date	2010
URL	http://hdl.handle.net/10722/124085
Rights	Published in ChemMedChem: chemistry enabling drug discovery, 2010, v. 5 n. 3, p. 468-475

Silver nanoparticles mediate differential responses in keratinocytes and fibroblasts during skin wound healing

Xuelai Liu[1], Pui-yan Lee[1], Chi-ming Ho[2], Vincent CH Lui[1], Yan Chen[1], Chi-ming Che[2], Paul KH Tam[1], Kenneth KY Wong[1*]

[1] Department of Surgery, LKS Faculty of Medicine, The University of Hong Kong, Pokfulam, Hong Kong

[2] Department of Chemistry, The University of Hong Kong, Pokfulam, Hong Kong

*Correspondence to: Dr. Kenneth Wong, Ph.D, FRCSEd, FHKAM

Department of Surgery,

The University of Hong Kong,

Queen Mary Hospital, Pokfulam Road,

Hong Kong SAR ,China.

Tel : +852 28553486

Fax : +852 28173155

Email: kkywong@hku.hk

ABSTRACT

Aims: With the advances in nanotechnology, pure silver has recently been engineered into nanosized particles with diameter less than 100 nm and utilized in the treatment of wounds. Together with other studies, we have previously demonstrated that topical application of silver nanoparticles (AgNPs) could promote wound healing through a modulation of cytokines. Nonetheless, the question of whether silver nanoparticles have the potential to affect various skin cell types - keratinocytes and fibroblasts, during the process of wound healing still remains. The aim of this study was therefore to focus on the cellular response and events of dermal contraction and epidermal re-epithelization during wound healing under the influence of nanosilver.

Materials & Methods: We employed a using a full-thickness excisional wound model in mice. The wounds were treated with either nanosilver particles or control with silver sulphadiazine. The proliferation and biological events of keratinocytes and fibroblasts during healing were studied.

Results: Our results confirmed that silver nanoparticles could increase the rate of wound closure. This was achieved, on one hand, through the promotion of proliferation and migration of keratinocytes. On the other hand, AgNPs could drive the differentiation of fibroblasts into myofibroblasts, thereby promoting wound contraction.

Conclusions: These findings have further extended our current knowledge of silver nanoparticles in biological and cellular events and also have significant implications

for the treatment of wounds in the clinical setting.

INTRODUCTION

Healing of wound is a complex and multiple-step process involving integration of activities of different tissues and cell lineages.[1] Re-epithelization, a crucial process during the early phase of wound healing, occurs not only by the migration and proliferation of keratinocytes in the epidermal layer of skin from the wound edge, but also by differentiation of stem cells residing in the bulge of hair follicle.[2] Rapid re-epithelization after wounding will provide an optimum environment, such as a scaffold of cells and various growth factors, which are indispensable in wound healing. Further to re-epithelialization, wound contraction is another important process in the early phase of wound healing. It minimizes the open area by pulling the neighboring tissue towards the wound center. In this process, alpha smooth muscle actins (α-SMA), generated from myofibrobalsts, play a vital role in wound contraction. Myofibroblasts differentiated from fibroblasts generate the contractile force, through which the wound area could contract during wound healing.[3-4] This process occurs faster than re-epithelialization because no cell proliferation is involved.[5] Thus, intensive research of developing new drugs and technologies, are being currently pursued, for the promotion of re-epithelization and wound contraction.

Although silver nitrate was used as a disinfecting agent for wounds as far back as World War I, the current use of silver agents has been reduced to topical silver sulfadiazine cream in the treatment of burn wounds because of the availability of excellent and effective antibiotics.[6-11] Renewed interest in silver only rekindled after

nanotechnology has made it possible to produce pure silver particles in the nano-scale. In the case of exposing cells or tissue to silver nanoparticles (AgNPs), the active surface would be significantly larger compared to silver compounds, and thereby exhibiting remarkably unusual physicochemical properties and biological activities.

In our previous work using a burn wound model in mice, we demonstrated that silver nanoparticles promoted wound healing through its powerful antibacterial property, as well as its ability to reduce inflammation.[12-13] Nonetheless, the observed findings were only the end result of the complex interplay between various resident skin cell types and the recruited inflammatory cells. The question thus remains on whether silver nanoparticles can have individual effects on various the skin cell types. This is particularly important in the wound healing process since re-epithelization and wound contraction represent two components mediated by two different cell types – keratinocytes and fibroblasts. In this study, we chose an excisional wound model because this model provided a relatively cleaner wound than the burn wound and therefore could reduce the potential effect of the infective factor. Furthermore, we could separate and observe more clearly the cellular events occurring in keratinocytes and fibroblasts during wound healing. Our results showed that silver nanoparticles could indeed mediate different events in keratinocytes and fibroblasts. On the one hand, there was an increase in the rate of proliferation of keratinocytes after wounding. In contrast, proliferation of fibroblasts was suppressed, but with subsequent drive towards differentiation into myofibroblasts. The findings

have further improved our existing knowledge in the action of silver nanoparticles on a cellular level and we also showed for the first time that this precious metal could have differential effects on different cell types.

MATERIALS AND METHODS

Animals

C57BL/6N aged between 6-8 weeks old, weighing between 16-22 grams were obtained from the Laboratory Animal Unit, The University of Hong Kong. The animals were allowed diet and water ad libitum in a 12-hour light, 12-hour dark cycled room. The experimental protocol was approved by the Committee of the Use of Live Animals in Teaching and Research, The University of Hong Kong (CULATR 1599-08). Anesthesia for experimentation was achieved with an intra-peritoneal injection of pentobarbital sodium solution (Abbott Laboratories, U.S.A) at a dose of 50 mg/Kg.

Nanosilver particles and other silver preparations

Nanosilver particles (AgNPs) were synthesized based on the following method. 10 mg of sodium borohydride was added into a 0.1 mM silver nitrate solution (1L), which contained 0.7 mM of sodium citrate, and the solution was stirred overnight. The reaction was monitored by UV-vis spectroscopy until no further absorption increase at 400 nm wavelengths. The solution was then reduced to 100ml by rotary evaporator. Final concentration of solution was 1 mM. The mean diameter of the

nanosilver particles was 10 nm (range 5 to 15nm) and confirmed by electron microscopy.

1% silver sulphadiazine (SSD) cream (Smith & Nephew Phamacenticals Ltd., USA) was used as control in animal experiments (silver content 3.02 mg/g). In in-vitro experiments, silver sulphadiazine powder ($C_{10}H_9AgN_4O_2S$; FW 357.14, 98%) was purchased from Sigma-Aldrich. The powder was added and dissolved thoroughly in sterile water to make a final concentration of 1 mM.

Wounding Protocol and Treatment

Mice were randomly divided into three groups, AgNPs group, SSD group and no treatment group (n=5). After anesthesia, the dorsal hair was shaved and cleansed with 10% w/V povidone iodine before a 1.5×1.5 cm^2 full-thickness wound was created surgically. In the AgNPs group, AgNPs solution coated dressing was topically applied to the wound bed, with the AgNPs concentration in each dressing equal to previously described (0.04 mg/cm^2).[13] In the SSD group, mice were treated by topical application of 30 mg 1% silver sulphadiazine cream, the same amount of silver as those in the AgNPs group. The wound dressings were changed daily until sacrifice or wound healing.

Morphometric assessment of wound re-epithelization and wound closure

Morphometric assessment of wound re-epithelization and wound closure was examined and documented daily using digital photography. The digital camera was

secured on a cantilever at a fixed distance. Wound areas (cm^2) were calculated from wound perimeter tracings using Photoshop CS® (Adobe, USA) in a single-blinded manner until the wound was completely healed. The healing rate was expressed as a percentage of the original dorsal wound area on day 0 after wounding ($1.5x1.5cm^2$). Thus:

$$\% \text{ Wound area} = \frac{\text{Wound area on day n}}{\text{Original wound area at day 0}} \times 100\%$$

Histological Examination

At various time points, mice from each group were sacrificed and the original wound areas were harvested, formalin-fixed and embedded in paraffin. 5 μm sections were microtomed, de-waxed and re-hydrated. Staining was performed with hematoxylin and eosin (H&E). In order to observe the extent of re-epithelization (migration of keratinocytes in nascent epidermal layer of skin), the harvested wound tissues were sectioned through the centre of the wounds, thereby incorporating areas from the centre to the original wound edge. Four photographs (40x) were taken and cells were counted, with the final data expressed from an average of four sections.

Cell culture

For in-vitro cell culture, mouse embryo fibroblast cell line (BALB/3T3; clone A31) was purchased from ATCC and was cultured as described. Briefly, fibroblasts were

seeded and grown in DMEM (Sigma, USA) with 10% FBS and penicillin/streptomycin mixture in 5% CO_2 at 37°C. The cultures were passaged twice before experiments.

Ex-vivo culture of keratinocytes and fibroblasts were obtained from the dorsal skins of mice after sacrifice. The skin was cleansed with 10% w/V povidone iodine and washed in the D-hanks solution 5 times and the subcutaneous tissues were removed. Each piece of skin (5cm x 5cm) was then cut into 0.5cm x 0.5cm fragments. 0.25 % dispase II (Sigma) was added to cover the skin fragments and left to digest at 4°C for 16 hours. The epidermis was peeled off for keratinocyte culture. The dermis tissue was put into a fresh dish for fibroblast culture. The epidermal tissues harvested were cultured in 8-well plates using epidermal keratinocyte medium with 10% fetal bovine serum. Dermal tissues harvested were cultured in 8-well plates using DMEM containing 10% fetal bovine serum. 100μl of AgNPs solution (50 μM) was added to wells, with SSD as the control. In each well, 10 random visual fields (100x) were chosen to calculate the outgrowth cell number.

Immunohistochemistry (IHC) and fluorescence staining

Healing wound tissues were harvested and processed as previously. The endogenous peroxidase was quenched by treated in 3% hydrogen peroxide/methanol for 10 min. Sections were incubated for 1 hour at room temperature with blocking solution containing 5% normal goat serum (Dako Bioresearch, USA). For antigen retrieval of alpha-SMA staining, the sections were further blocked for nonspecific binding with

10% normal goat serum before primary antibody (anti-α-SMA, Abcam Ltd, USA)
(1:100) was added. The sections were incubated overnight at 4°C before rinsing in
PBS, and then incubated with HRP-conjugated secondary antibody (Santa Cruz,
USA) for 1 hour. Positive signals were developed using DAB (3,3'-diaminobenzide
tetrahydrochloride) and counterstained with hematoxylin. FITC-conjugated goat
anti-mouse antibody was used as the secondary antibody for PCNA (PC10, Santa
Cruz, USA) (1:200) for fluorescence staining. The tissues were washed three times
in 1x PBS and stained with DAPI prior to microscopy.

For immunostaining of type I collagen and α-SMA in cell culture, fibroblasts grown
in chambers and mounted on glass slide with cover. AgNPs or SSD was added to the
medium to make concentration of 50 μM. The cells were incubated for 48 hours and
fixed in 4% paraformaldehyde. Samples were then washed with 0.25% Trion X-100
(Sigma). 1% BSA was used to block non-specific binding before the addition of
anti-α-SMA antibody (Abcam Ltd, USA) (1:100) or anti-type I collagen antibody
(Abcam Ltd, USA) (1:100). TRITC-conjugated goat anti-mouse antibody (1:200)
and TRITC-conjugated goat anti-rabbit antibody (1:200) were respectively used as
the secondary antibody. The samples were washed three times and incubated on
DAPI for 1 minute. Images were viewed under microscopy.

Hydroxyproline (Hyp) detection

For the determination of the hydroxyproline concentration, Medugorac's method was
performed.[14] The collagen content in supernatant was estimated from the

hydroproxyline concentration by multiplying its value by 7.46. Hydroxyproline (Hyp) kit was purchased from JianChen Gene Company (Nanjing, PR China) to detect the production of Hyp and content of collagen in supernatant. 0.875×10^5 cells were seeded in 1 ml DMEM (Sigma, USA) with 10% FBS and penicillin/streptomycin mixture on each well of 6 well-plate in 5% CO_2 at 37°C and incubated for 24 hours. Treatment with various concentrations of silver nanoparticles was added and then incubated for 2 days. Supernatant in each well was collected and made in triplicates for test tubes. 250μl of supernatant and 50μl digestive solution were added to the test tubes and incubated for 3 hours in 37°C warm bath. Then, 500μl of isopropanol, 500μl of oxidant of solution, 1 ml of 7% trihydrated chloramine-T solution were added. These were mixed well and incubated for 15 minutes at 60°C. The tubes were centrifuged at 3500rpm for 10 minutes at room temperature. The absorbance in each tube was measured at 550 nm in a microtiter plate reader (Bio-Rad Inc, USA). The average values from triplicate readings were calculated.

MTT assay

Cell proliferation assay kit (Roche, Germany) was used to measure cell proliferation rate and reduction in cell viability during apoptosis or necrosis. 2×10^3 cells were plated out, in triplicate, into wells of a microtiter plate. Three control wells with medium alone were used to provide blanks for absorbance readings. Treatment with various concentrations of silver nanoparticles was added, followed by 100 μL of MTT Reagent to each well, including controls. When purple precipitate was clearly visible

under the microscope, 100 μL of Detergent Reagent was added to all wells, including control. The plate was covered and left in the dark for overnight in 37°C incubator. The plate cover was removed and the absorbance in each well was measured at 570 nm in a microtiter plate reader (Bio-Rad Inc, USA). The average values from triplicate readings were calculated and the blank was subtracted from the average value.

Statistic analysis

Statistical analyses were performed using Student's paired t-test. A p value of < 0.05 was considered significant.

Results

Accelerated wound closure by silver nanoparticles in early phase of wound healing

The earliest histological change in the wound bed after wounding is wound contraction. This is a vital process to minimize open wound area. Wound contraction is effected through activated fibroblasts located on the wound edge. These differentiate into the myofibroblasts, which will secret actins and elastic fibers for wound contraction. In order to assess the wound-contraction rate, we measured the percentage of wound bed area at various time points until complete wound closure. In our model, untreated wounds closed after 28.1±1.60 days. In mice treated with silver nanoparticles, this event took only 18.4±1.26 days, while wounds closed in 24±0.67 days in animals treated with silver sulphadiazine ($p<0.01$) (Figures 1

A&B).

We next calculated the rate of wound closure using the formula described previously. As can be seen in Figure 1C, the rate of wound closure in the AgNPs group from day 9 post wounding significantly increased when compared with control (p<0.01), with the wound area decreased to 31.23% of original size as early as day 12 and to 3.34% on day15. These observations further confirmed that silver nanoparticles could accelerate the wound closure.

Silver nanoparticles promote re-epithelization through increased keratinocyte migration and proliferation

After wounding, although the myofibroblasts (differentiated from fibroblasts) and the extracellular matrix provide the necessary environment for wound contraction, it is the proliferation and migration of keratinocytes from the wound edge that provide cells for wound covering through re-epithelization (Figure 2A). We therefore asked whether silver nanoparticles could exert their effects on the proliferation of keratinocytes, and thus re-epithelization. First, histological sections taken from day 7 wounds were studied. Although H&E staining showed that the epithelium at the wound edge of all wounds migrated towards the centre, the epithelial tongue (indicated by the vertical line) in AgNPs group was found to move faster than controls (Figure 2B). The same phenomenon was observed when the extent of growth of the epithelial tongues was measured at three different time points (Figure 2C) (*p*<0.01). Using immunohistochemistry to stain for cell divisions in epithelial

tongue area, we further confirmed that there was an increase in cell proliferation in animals treated with AgNPs (Figure 2D). The average number of proliferating keratinocytes in each group obtained by counting in five random visual fields under the microscope also showed significantly more proliferating keratinocytes in the AgNPs group than in the other two groups (Figure 2E) ($p < 0.01$). Histological examination performed on the healed wounds showed also that AgNPs group showed the closest resemblance to normal skin (Figure 2F).

Taken these findings together, although we found a higher density of proliferating cells in the epidermal layer in the AgNPs group during the healing phase, the fact that the overall histology of the healed skin resembled that of normal epithelium would suggest that silver nanoparticles could trigger the maturation of the proliferating keratinocytes.

Enhanced keratinocyte outgrowth and inhibited fibroblast proliferation by silver nanoparticles

In order to further understand the possible individual action of silver nanoparticles on various skin cell types separately, keratinocytes and fibroblasts were isolated, and cultured ex-vivo. After the addition of AgNPs to the culture medium, we found a significant increase in keratinocyte proliferation when compared to control (Figure 3A). Furthermore, this effect appeared to sustain for up to 7 days (Figure 3B).

In contrast, when fibroblasts were cultured ex-vivo, there was a reduction in the cell number in the presence of AgNPs (Figures 3 C&D) ($p < 0.01$).

To determine if the reduction in fibroblast number was due to toxicity of AgNPs, MTT assay was performed. Our results here demonstrated that at 100μM or less, AgNPs was relatively non-toxic to fibroblasts (Figure 4A). Furthermore, when we determined the level of production of hydroxyproline and collagen in fibroblasts, we showed that silver nanoparticles could significantly decrease the production of these proteins in the supernatant (Figure 4B-D). This would suggest that the addition of silver nanoparticles could change the normal phenotype of the fibroblasts.

Differentiation of myofibroblasts from fibroblast driven by silver nanoparticles

When one looks more closely at the events duing wound healing, wound contraction certainly plays a significant role. We therefore asked whether the effects of silver nanoparticles on fibroblasts could be due to the differentiation of fibroblasts into myofibroblasts, with a consequent decrease in cell proliferation.

Here, we stained cultured fibroblast for collagen I and α-SMA after the addition of sivler nanoparticles. As shown in figure 5A, there was a marked reduction of collagen I expression. On the other hand, the expression of α-SMA was markedly increased (Figure 5B). Taken together, it would suggest a change in phenotype from fibroblasts to myobibroblasts.

To further confirm this finding in vivo, we next took wound sections from our experimental animal groups and stained for α-SMA, a marker for myofibrobalsts. Normally, α-SMA could only be detected in small amount in normal skin. Here, the amount of α-SMA in day 7 wounds in the AgNPs group was significant more when

compared to the control groups. (Figure 5C). Thus, it would appear that silver nanoparticles could indeed drive the differentiation of resident fibroblasts into myofibroblasts in the early phase of wound healing, thereby help to accelerate wound bed contraction.

Discussion

The antibacterial action of silver has been known since ancient times. As a result, this precious metal has long been utilized to treat infectious diseases. Despite this, only recently have researchers been beginning to unravel some of the mechanisms of action of silver. It exerts its antibacterial property by interfering with the respiratory chain of the cytochromes and components of the microbial electron transportation system, and also binds and inhibits bacteria DNA replication.[15-17] Others have found that silver nanoparticles had anti-bacterial and anti-inflammatory properties in infectious wound.[18] Nevertheless, the mechanism of action of silver on wound healing remains unresolved. In our previous study, we showed that topically delivered silver nanoparticles promoted wound healing in a burn wound model through their effective antibacterial properties. Furthermore, it appeared that silver could modulate cytokine production.[12] In the burn model, it was relatively difficult to observe the re-epithelization process and other effects exerted by silver on a cellular level during wound healing because of cellular destruction from the burn injury. To further clarify and dissect out any possible effects of silver nanoparticles on various cell types, we adopted a surgical wound on dorsal skin in

mouse. The clean and infection free wound would make it possible to observe the morphological change during re-epithelization and wound contraction.

In this study, we found that, as in the burn wound model, animals treated with silver nanoparticles had significantly faster wound closure when compared to the silver sulphadiazine group. This result further confirmed the beneficial effects of silver nanoparticles, as a treatment for skin wounds. Furthermore, our results would suggest that silver in the nano form was a more effective drug than silver compounds for wound healing treatment, even when infectious and inflammatory factors were eliminated. Our previous study already showed that the addition of silver nanoparticles to the wound would reduce both local, as well as systemic inflammation, and resulted in faster healing. However, the effect of nanosilver on various skin cell types at a biological level is yet unclear. As wound healing involves re-epithelization process and wound contraction, it would be prudent to study any possible effects of nanosilver on individual cell types. Re-epithelization is a complex and multistep process, which involves keratinocyte migration and proliferation in the epidermal layer.[5, 19-20] In addition, wound contraction, a cellular event which occurs in the dermal layer through myofibrobalsts, minimizes the open wound bed by pulling the neighboring tissue towards the wound center. A few studies looking into wound healing events have shown that many drugs could promote wound healing by accelerated re-epithelization via enhanced keratinocyte migration and proliferation.[21-24] In our study, we firstly focused on the keratinocytes to investigate the morphological change mediated by silver

nanoparticles. In agreement with others, our histological finding demonstrated that silver nanoparticles indeed promoted proliferation and migration of keratinocytes from wound edge towards the wound center. This was further confirmed in our ex-vivo wound model experiment, using keratinocytes from peeled fresh epidermis.

Apart from faster healing, we also observed from histological evaluation that the healed wounds of animals in the silver nanoparticles group resembled closely to normal skin, with relatively thin epidermis and normal hair follicles. Taken together, it would suggest that silver nanoparticles could trigger the differentiation and maturation of keratinocytes, although at this point, the underlying mechanism through which silver operates is still unclear. One possibility may be the Notch signaling pathway, which is one of the most conserved and commonly used communication channels in animal cells. Studies have demonstrated this pathway is indispensable for cells in various stages of maturation, including terminal differentiation of keratinocytes.[25-26] As a result, further studies are currently underway to ascertain if silver does interact with Notch or its ligands. Indeed, as keratinocytes arise from the epidermal stem cells, there is also a possibility that silver nanoparticles can promote the differentiation and maturation of keratinocytes through the stimulation of skin stem cell.[27-30] This is an important issue because the ability to manipulate stem cells would open a new dimension in terms of tissue regeneration in the future.

On the other hand, although fibroblasts have been targets of intense research in the formation of keloid and hypertrophic scars, their role in the process of wound

healing has largely been neglected.[31-38] In our study, we also focused on the fibroblasts in the dermal layer. As our ex-vivo experiments clearly showed, in contrast to the effects seen in keratinocytes, the addition of silver nanoparticles suppressed the proliferation of fibroblasts. For this finding, we further confirmed that the suppression was not due to the toxic effects of silver. Looking back at the results on keratinocytes, it would appear that silver nanoparticles could drive differentiation and maturation. We therefore asked if the same effect could be seen in fibroblasts. Indeed, the decreased level of collagen in fibroblasts treated with nanosilver already would suggest that this could be the case. This was further confirmed by the increased expression of α-SMA, a marker of myofibroblast, both in in-vitro, as well as in-vivo experiments. This would suggest, as in the case of keratinocytes, that silver nanoparticles could indeed stimulate cell maturation, and hence, driving fibroblasts into myofibrobalsts during healing. Taken all the evidence taken together, we can now explain, at least at the cellular level, the reason why silver nanoparticles could significantly promote wound healing. It would seem that both wound re-epithelializaion and contraction are increased through the differential effects of silver on keratinocytes and fibroblasts. Despite this, how silver interacts at the molecular level during wound healing still remains to be determined. Microarray analyses are currently ongoing in our laboratory to try to unravel this mystery and identify the signaling pathways involved.

In addition to the beneficial effects on wound healing, the reduction of collagen production in fibroblasts by silver nanoparticles may suggest a role in anti-fibrosis

therapy, which could be useful in preventing and perhaps treating keloids and scars. If indeed this were to be the case, silver nanoparticles could prove to be the Holy Grail for wound healing without scars. In conclusion, our study further confirmed the significantly beneficial effects of silver nanoparticles on wound healing and for the first time, provided the evidence that silver could act on keratinocytes and fibroblasts. This has further enhanced our knowledge of the biological events exerted by this precious metal.

References

[1] P. Martin, *Science* **1997**, 276, 75-81.

[2] H. Nagato, Y. Umebayashi, M. Wako, Y. Tabata, M. Manabe, *Journal of Dermatology* **2006**, 33, 670-675.

[3] J.V. Jester, W.M. Petroll, H.D. Cavanagh HD, *Prog Retin Eye Res* **1999**, 18, 311–356.

[4] J.E. Feugate, Q. Li, L. Wong, M. Martins-Green, *J Cell Biol* **2002**, 156, 161–172.

[5] P.Y. Lee, S. Chesnoy, L. Huang, *J Invest Dermatol* **2004**, 123, 791 –798.

[6] C.S. Chu, A.T. McManus, B.A. Pruitt, A.D. Mason, *J Trauma* **1988**, 28, 1488–92.

[7] E.A. Deitch, A. Marin, V. Malakanov, J.A. Albright, *J Trauma* **1987**, 27, 301–4.

[8] H.W. Margraff, T.H. Covey, *Arch Surg* **1977**, 112, 699–704.

[9] D. Wyatt, D.N. McGowan, M.P. Najarian, *J Trauma* **1990**, 30, 857–65.

[10] X. Chen, H.J. Schluesener, *Toxicology Letters* **2008**, 176, 1–12.

[11] D.M. Caruso, K.N. Foster, S.A. Blome-Eberwein, J.A. Twomey, D.N. Herndon, A. Luterman, P. Silverstein, J.R. Antimarino, G.J. Bauer, *J Burn Care Research* **2006**, 27, 298-309.

[12] J. Tian, K.K. Wong, C.M. Ho, C.N. Lok, W.Y. Yu, C.M. Che, J.F. Chiu, P.K. Tam, *ChemMedChem* **2007**, 2, 129 -136.

[13] K.K. Wong, S.O. Cheung, L.M. Huang, J. Niu, C. Tao, C.M. Ho, C.M. Che, P.K. Tam, *ChemMedChem*. **2009**, 4,1129-35.

[14] I. Medugorac, *Res Exp Med (Berlin)* **1980**, 177, 201-11.

[15] P.D. Bragg, D.J. Rainnie, *Can J Microbial* **1974**, 20, 883-89.

[16] S.M. Modak, C.L. Fox, *Biochem Pharmacol* **1973**, 22, 2391-404.

[17] H.S. Rosenkranz, S. Rosenkranz, *Antimicrob Agents Chemother* **1972**, 2, 373-83.

[18] K. Dunn, Y. Edwards-Jones Y, *Bums* **2004**, 30 Suppl. 1, S1-S9.

[19] S.A. Eming, S. Werner, P. Bugnon, C. Wickenhauser, L. Siewe, O. Utermöhlen, J.M. Davidson, T. Krieg, A. Roers, *Am J Path* **2007***, 170, 188-202.

[20] P.Y. Lee, E. Cobain, J. Huard, L. Huang, *Molecular therapy*. **2007**, 15, 1189–1194.

[21] M. Tomic-Canic, S.W. Mamber, O. Stojadinovic, B. Lee, N. Radoja, J. McMichael, *Wound Repair Regen.* **2007**, 15, 71-9.

[22] T.T. Phan, M.A. Hughes, G.W. Cherry, *Wound Repair Regen.* **2001**, 9, 305-13.

[23] M. Carretero, M.J. Escámez, M. García, B. Duarte, A. Holguín, L. Retamosa, J.L. Jorcano, M.D. Río, F. Larcher, *J Invest Dermatol.* **2008**, 128, 223-36.

[24] C. Valencia, J. Bonilla-Delgado, K. Oktaba, R. Ocadiz-Delgado, P. Gariglio, L. Covarrubias, *J Invest Dermatol.* **2008**, 128, 2894-903.

[25] S. Chiba, *Stem cell* **2006**, 24, 2437–2447.

[26] B.J. Nickoloff, J.Z. Qin, V. Chaturvedi, M.F. Denning, B. Bonish, L. Miele, *Cell Death Differ.* 2002, 9, 842-55.

[27] J. Cha, V. Falanga, *Clin Dermatol.* **2007**, 25, 73-8.

[28] G. Cotsarelis, *J Invest Dermatol.* **2006**, 126, 1459-68.

[29] S. Tiede, J.E. Kloepper, E. Bodo, S. Tiwari, C. Kruse, R. Paus, *Eur J Cell Biol.*

2007, 86, 355-76.

[30] A.A. Panteleyev, C.A. Jahada, A.M. Christiano, *J Cell Sci.* **2001**, 114(Pt 19), 3419-31.

[31] Y. Chu, F. Guo, Y. Li, X. Li, T. Zhou, Y. Guo Y, *Connect Tissue Res* **2008**, 49, 92-8.

[32] A. Thielitz, R.W. Vetter, B. Schultze, S. Wrenger, L. Simeoni, S. Ansorge, K. Neubert, J. Fause, P. Lindenlaub, H.P. Gollnick, D. Reinhold, *J Invest Dermatol* **2008**, 128, 855-66.

[33] W.S. Wu, F.S. Wang, K.D. Yang, C.C. Huang, Y.R. Kuo, *J Invest Dermatol* **2006**, 126, 1264-71.

[34] J.F. Liu, Y.M. Zhang, C.X. Yi, J.M. Sun, W.W. Li, *Zhonghua Zheng Xing Wai Ke Za Zhi* **2004**, 20, 265-7.

[35] A.M. Bernstein, S.S. Twining, D.J. Warejcka, E. Tall, S.K. Masur, *Mol Biol Cell* **2007**, 18, 2716-27.

[36] V. Barbaro, E. Di Iorio, S. Ferrari, L. Bisceglia, A. Ruzza, M. De Luca, *Invest Ophthalmol Vis Sci* **2006**, 47, 5243-50.

[37] T.P. Amadeu, B. Coulomb, A. Desmouliere, A.M. Costa, *Int J Low Extrem Wounds* **2003**, 2, 60-8.

[38] M.B. Vaughan, E.W. Howard, J.J. Tomasek, *Exp Cell Res.* **2000**, 257, 180-9.

Figure legends

Figure 1 – The effects of silver nanoparticles on wound healing. Excisional skin wounds were created on the dorsum of mice and they were divided in 3 groups (n=5) and received nanosilver particles, silver sulphadiazine or no treatment respectively. The wounds were inspected daily and the rate of healing was recorded. A. The time to complete wound closure in each group. (** $p<0.01$; *** $p< 0.001$) B. Photographs of wound appearance from three groups at various time points. C. The rate of wound closure at various time points after wounding.

Figure 2 - Re-epithelization and proliferation of keratinocytes mediated by the silver nanoparticles during healing.

A. Schematic drawing of a wound indicating the location of proliferating cells examined. Region 1 represents the re-epithelization area and region 2 represents the epithelial tongue. B. The wounds were excised and stained with H&E on day 7 after wounding and the degree of wound closure was examined histologically. Proliferating cells arising form wound edge on the left migrated towards to the wound centre on the right. The blue bar indicates the leading edge of the epithelium. C. The extent of re-epithelization on day 7, day 10, and day 15 after wounding was measured histologically in three groups and represented (* $p<0.05$, ** $p<0.01$). D. immunohistochemistry staining of proliferating cells in the epithelial tongue area on day 15 after wounding. Dash line indicates the divison between the epithelial layer and the dermal layer. Scale bar: 20 um. E. Average numbers of proliferating cells in

epithelial tongue area on day 15 sample after wounding   (** p<0.01; *** P< 0.001)

F. Histological morphology of healed wounds in animals from the three groups.

Figure 3 - The effects of AgNPs on keratinocytes and fibroblasts in culture.

Keratinocytes and fibroblasts were obtained from the dorsal skins of mice, digested with 0.25 % dispase II, and cultured in appropriate media with either AgNPs or SSD. The number of cells in the outgrowth area was counted in each well and averaged.

A. The number of keratinocytes growing out from the epidermal margin in three groups after 2 days culturing (Scale: 100 um). B. Keratinocyte numbers in the outgrowth area counted and averaged at 6 time points. C. The number of fibroblasts grown from the dermal margin in three groups after 2 days culturing (Scale: 100 um). D. Fibroblast numbers in the outgrowth area at 6 time points.

Figure 4 – The effects of AgNPs on fibroblasts apoptosis and protein production.

Mouse embryo fibroblast cell line (BALB/3T3; clone A31) was cultured in medium with the addition of AgNPs for 24 hours and the effects on cell death and protein (collagen and hydroxyproline) were studied.

A. Viability of BALB/3T3 cells treated with AgNPs at a concentration range from 10 to 400 uM is expressed as percentage of untreated cells. Values are the mean±SE. (** p<0.01) B. Hyp content in supernatants of BALB/3T3 cells under different AgNPs concentration after 24 hours culture. The concentration was measured using

absorbance readings. C. Collagen content of BALB/3T3 cells in different AgNPs concentrations.

Figure 5 - Stimulated differentiatiation of fibroblast into myofibroblasts mediated by silver nanoparticles.

A. 3T3 fibroblasts cell line was cultured and treated with SSD and AgNPs and the level of collagen I was measured using immunohistochemistry.

B. Staining for myofibroblasts using α-SMA after culturing 3T3 fibrobalsts with AgNPs or SSD for 48 hours. (Red: α-SMA; Blue: nuclear of fibroblasts; Scale bar: 40 um).

C. α-SMA staining on Day 7 wounds of animals treated with either AgNPs or SSD and a comparison to normal skin. (Scale bar (left): 40 um. Scale bar (right): 20 um)

Fig 1A

Fig 1B

28

Fig 1C

Fig 2A

AgNPs

SSD

No treatment

Fig 2B

Fig 2C

	PCNA	DAPI	Merge
AgNPs			
SSD			
No Treatment			
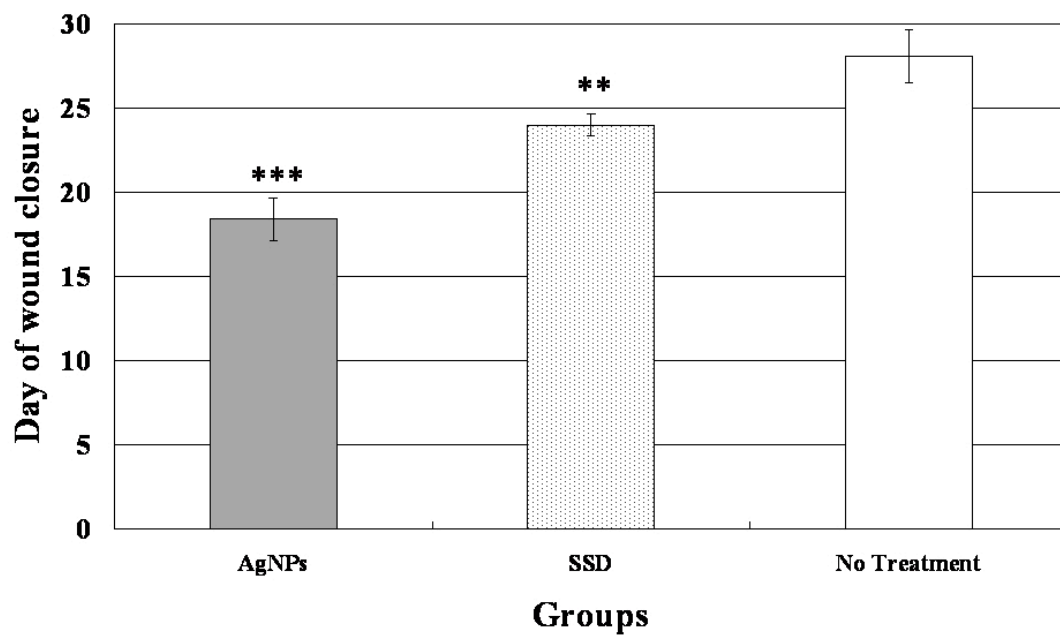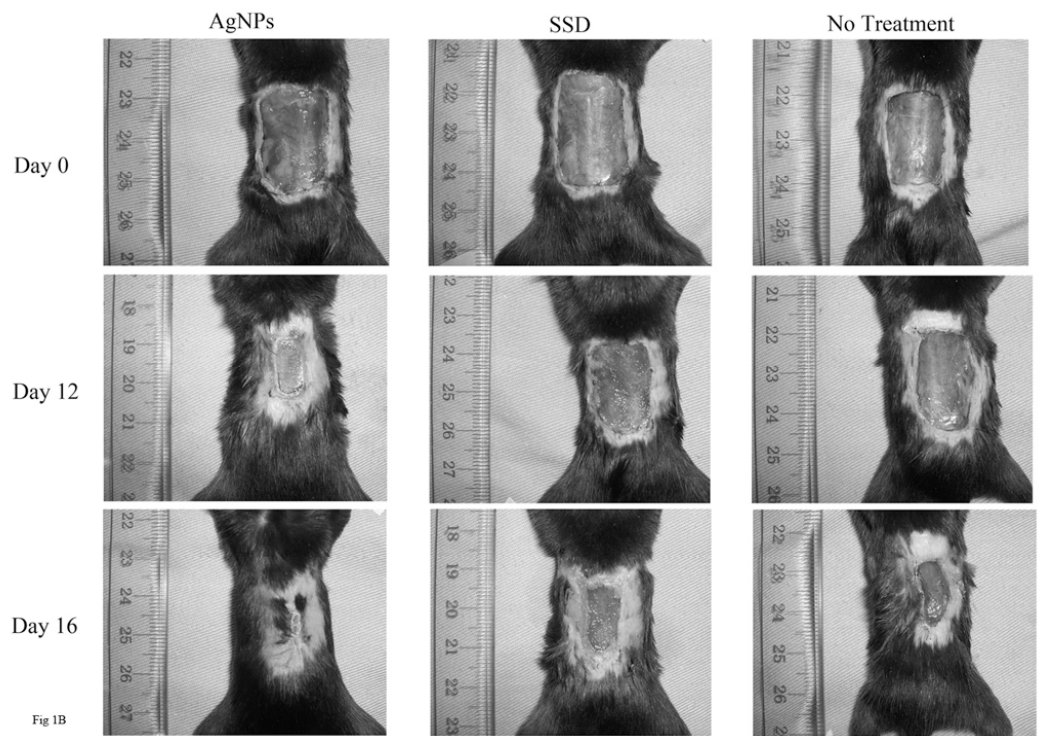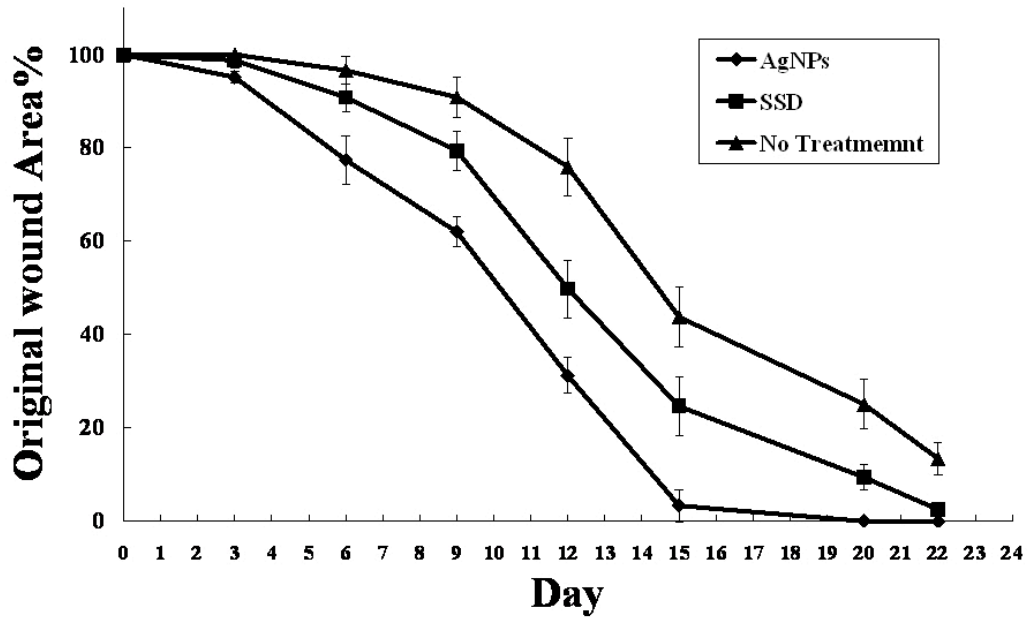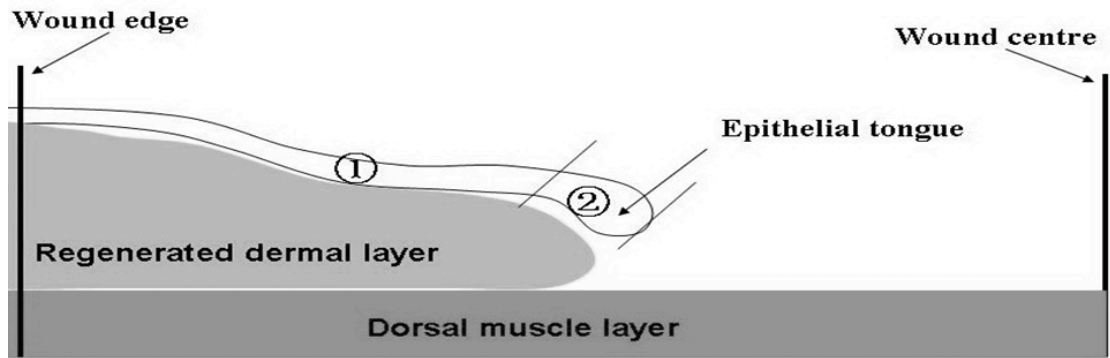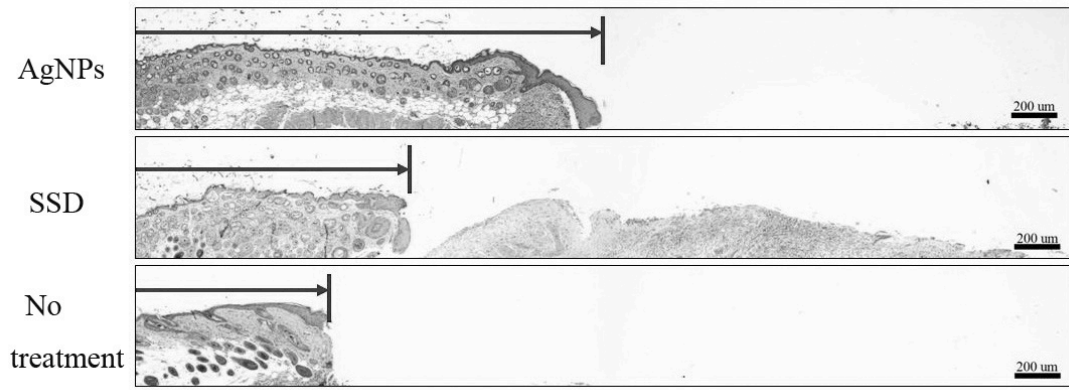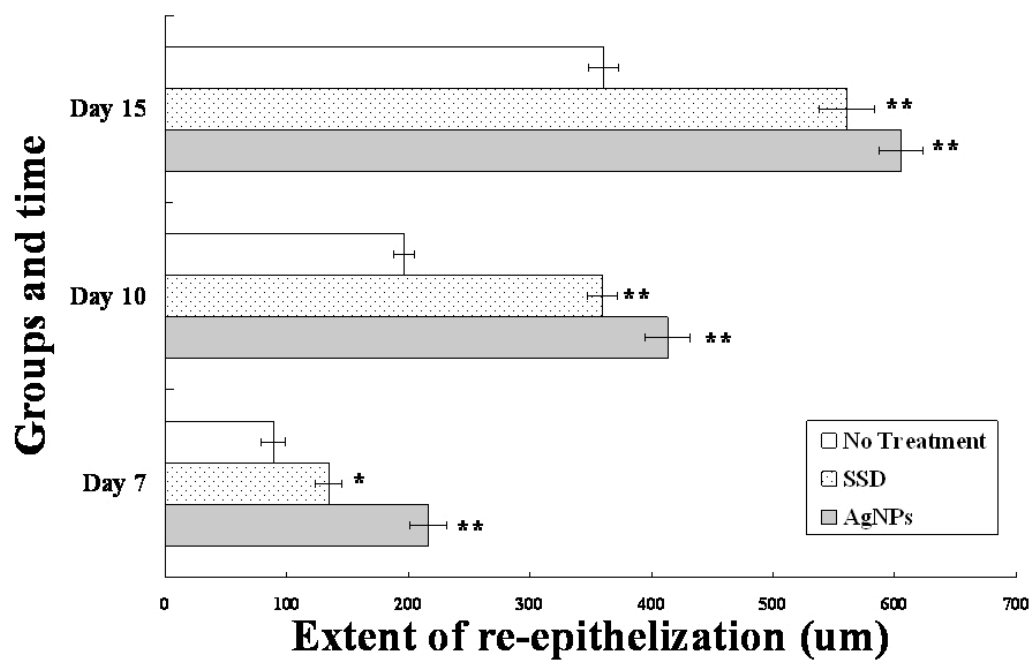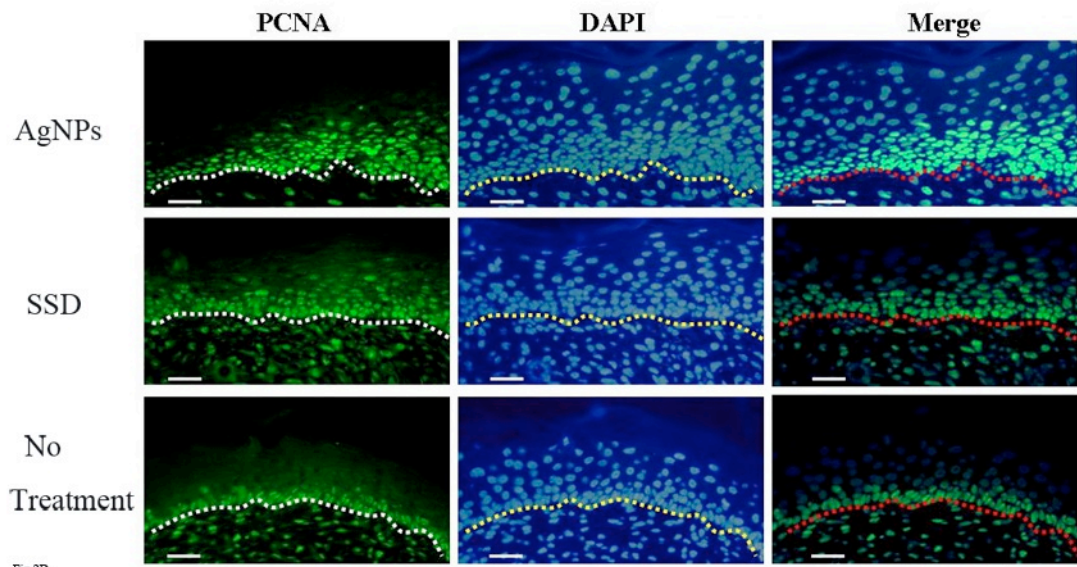
Fig 2D
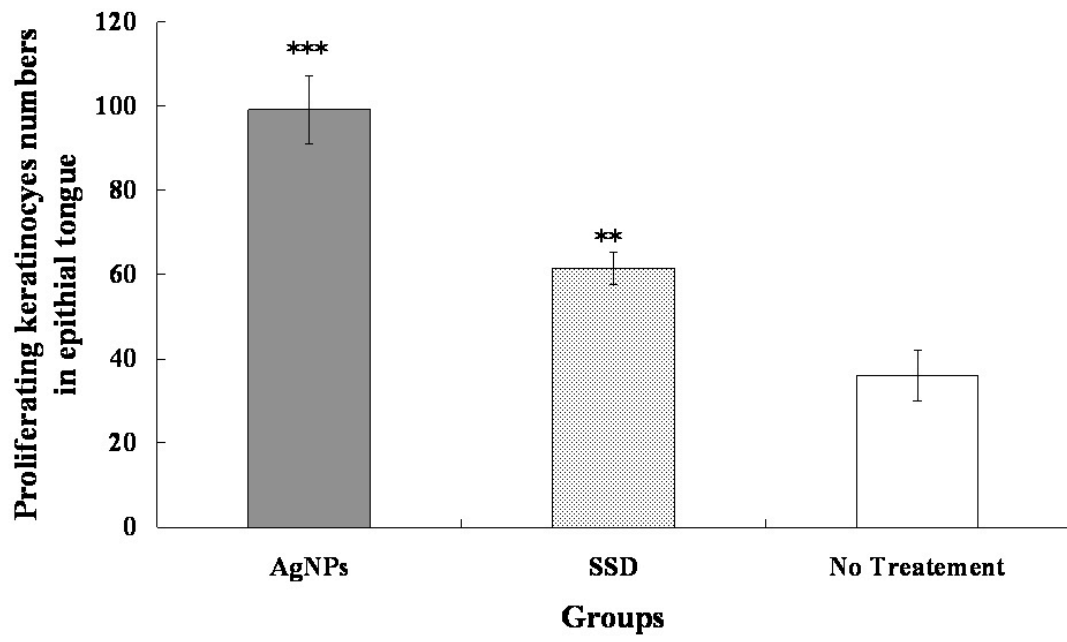
Fig 2E

Normal skin

AgNPs

SSD

No Treatment

Fig 2F

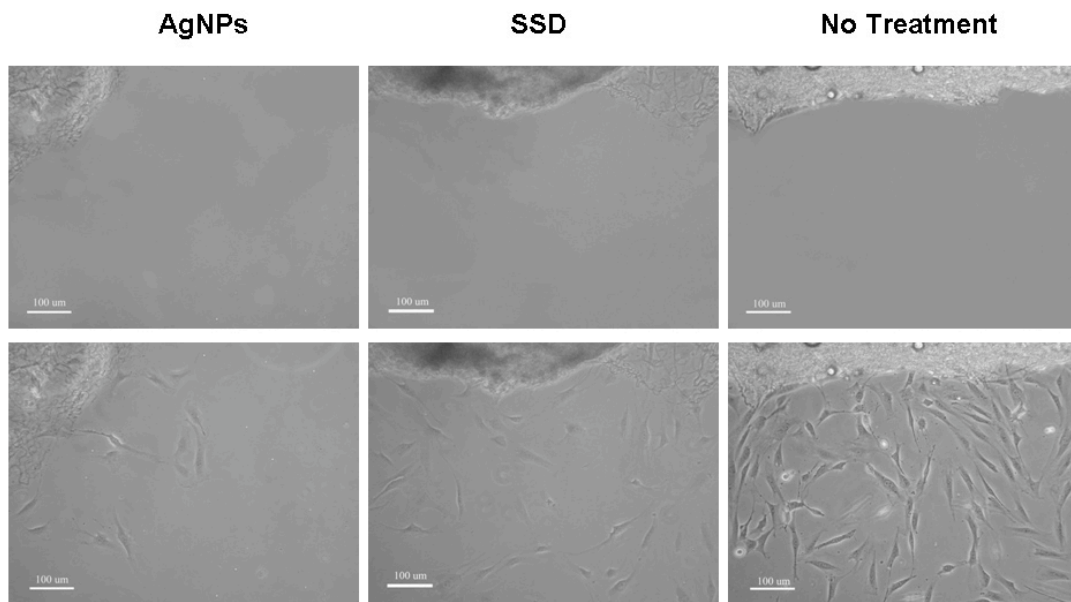| | AgNPs | SSD | No Treatment |

100 um (scale bars on each panel)
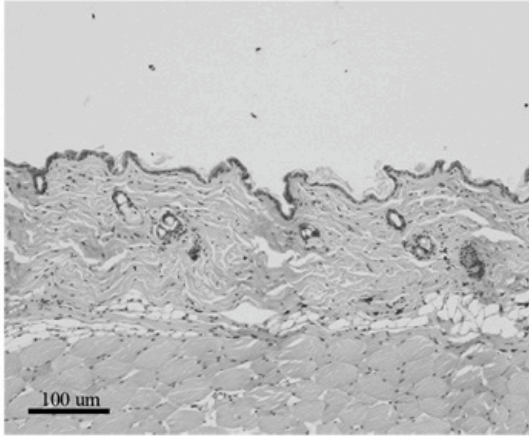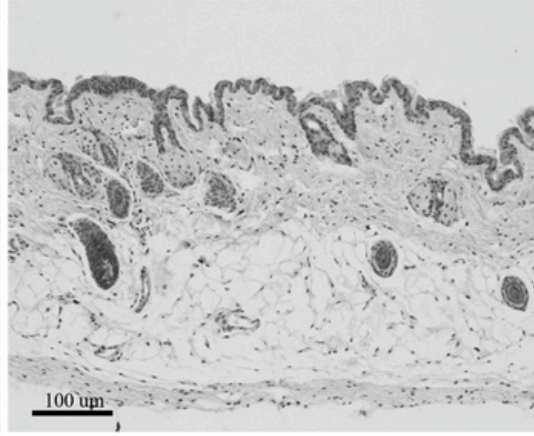
Fig 3A

Fig 3B

| AgNPs | SSD | No Treatment |
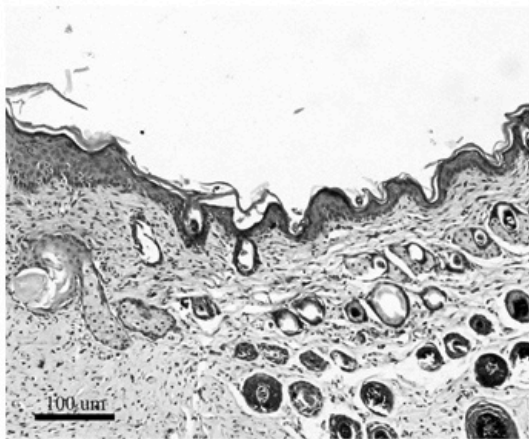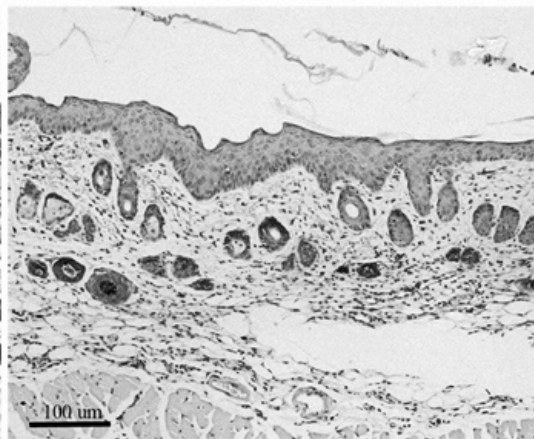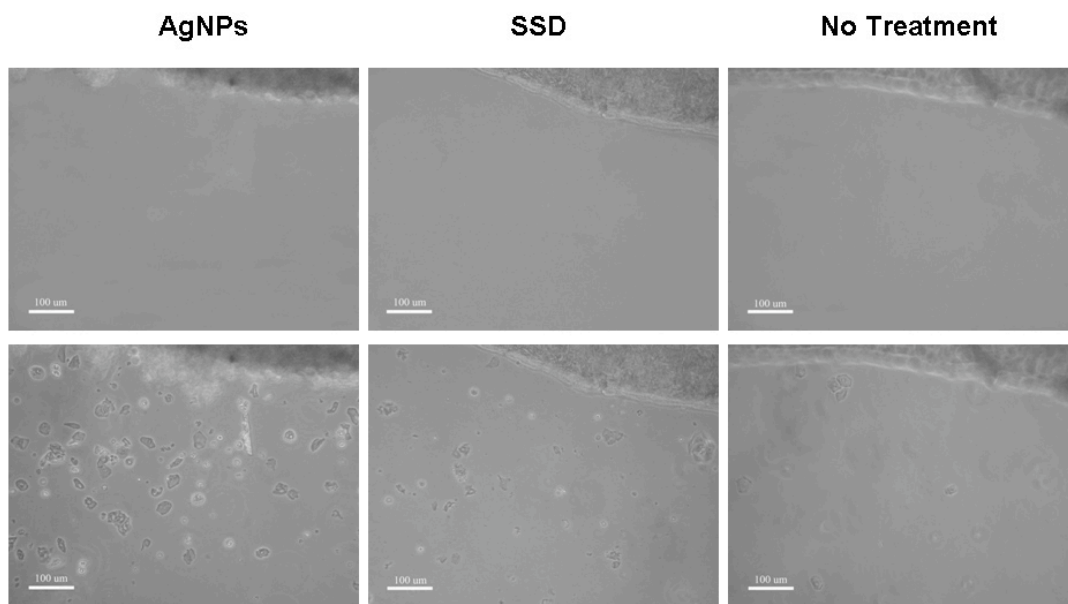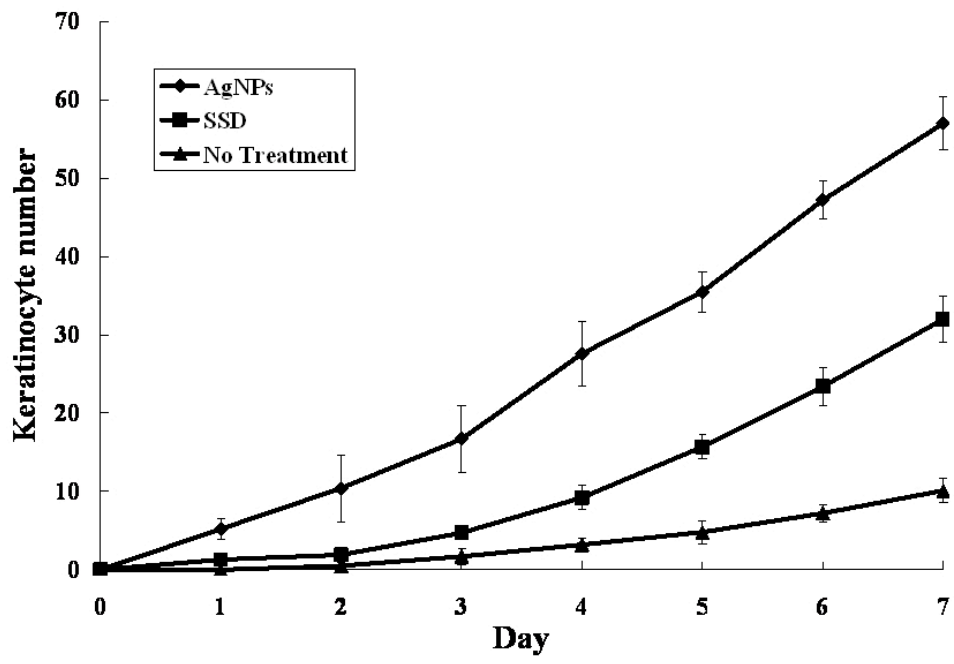
Fig 3C

Fig 3D

Fig 4A

Fig 4B

Fig 4C

	No Treatment	SSD (50 uM)	AgNPs (50 uM)	AgNPs (100 uM)
Collagen I				
DAPI				
Merge				

α-SMA   DAPI   Merge

AgNPs

SSD

No
Treatment

Fig 5B

Normal Skin

No Treatment

SSD

AgNPs

Fig 5C